HAL
open science

First Responders Shape a Prompt and Sharp NF-κB-Mediated Transcriptional Response to TNF-α

Samuel Zambrano, Alessia Loffreda, Elena Carelli, Giacomo Stefanelli, Federica Colombo, Edouard Bertrand, Carlo Tacchetti, Alessandra Agresti, Marco Bianchi, Nacho Molina, et al.

To cite this version:

Samuel Zambrano, Alessia Loffreda, Elena Carelli, Giacomo Stefanelli, Federica Colombo, et al.. First Responders Shape a Prompt and Sharp NF-κB-Mediated Transcriptional Response to TNF-α. iScience, 2020, 23 (9), pp.101529. 10.1016/j.isci.2020.101529 . hal-03044483

HAL Id: hal-03044483

https://hal.science/hal-03044483

Submitted on 9 Dec 2020

HAL is a multi-disciplinary open access archive for the deposit and dissemination of scientific research documents, whether they are published or not. The documents may come from teaching and research institutions in France or abroad, or from public or private research centers.

L'archive ouverte pluridisciplinaire **HAL**, est destinée au dépôt et à la diffusion de documents scientifiques de niveau recherche, publiés ou non, émanant des établissements d'enseignement et de recherche français ou étrangers, des laboratoires publics ou privés.

First responders shape a prompt and sharp NF-κB –mediated transcriptional response to TNF-α

Samuel Zambrano[1,2,3,4,*], Alessia Loffreda[5], Elena Carelli[4,6], Giacomo Stefanelli[5], Federica Colombo[4], Edouard Bertrand[7], Carlo Tacchetti[3,5], Alessandra Agresti[4], Marco E. Bianchi[3,4], Nacho Molina[8,*], Davide Mazza[2,5,*].

[1] Lead contact.
[2] These authors contributed equally.
[3] School of Medicine, Vita-Salute San Raffaele University, Milan, 20132, Italy.
[4] Division of Genetics and Cell Biology, IRCCS San Raffaele Scientific Institute, Milan, 20132, Italy.
[5] Experimental Imaging Center, IRCCS San Raffaele Scientific Institute, Milan, 20132, Italy.
[6] Current address: INGM-National Institute of Molecular Genetics "Romeo ed Enrica Invernizzi", Milan, 20100, Italy.
[7] Institut de Génétique Moléculaire de Montpellier, CNRS, Montpellier, 34293, France.
[8] Institut de Génétique et Biologie Moléculaire Cellulaire, Illkirch-Graffenstaden, 67404, France.

* Correspondance to : SZ: Zambrano.samuel@hsr.it; DM: mazza.davide@hsr.it; NM, for stochastic inference algorithms: nacho.molina@igbmc.fr.

Summary

NF-κB controls the transcriptional response to inflammatory signals by translocating into the nucleus, but we lack a single-cell characterization of the resulting transcription dynamics. Here we show that transcription of NF-κB target genes is heterogeneous in individual cells but yet results in an average nascent transcription profile that is prompt (i.e. occurs almost immediately) and sharp (i.e. increases and decreases rapidly) compared to NF-κB nuclear localization. Using an NF-κB-controlled MS2 reporter we show that the single-cell nascent transcription is more heterogeneous than NF-κB translocation dynamics, with a fraction of synchronized "first responders" that shape the average transcriptional profile and are more prone to respond to multiple TNF-α stimulations. A mathematical model combining NF-κB mediated gene activation and a gene refractory state is able to reproduce these features. Our work shows how the expression of target genes induced by transcriptional activators can be heterogeneous across single cells and yet time-resolved on average.

Introduction

A tight control of gene expression is assumed to be fundamental for any living system, from prokaryotes to higher organisms. For this reason, it was surprising to find that the same gene within a clonal population of identical cells can be translated into different protein levels (Ko et al., 1990) which can fluctuate in time even within the same cell (Elowitz et al., 2002). The development of accurate techniques allowing to measure gene expression in single living cells showed that such variability is related to discontinuous transcriptional "bursts" (Tunnacliffe and Chubb, 2020), spurts of RNA production interspersed with periods of no activity, that emerge from fluctuations of the gene between "active" and "inactive" states whose precise origin is only partially understood (Chong et al., 2014).

Transcriptional bursts have been observed for a variety of organisms (Golding et al., 2005; Pichon et al., 2018; Suter et al., 2011), but their functional role is also unclear, although it has been proposed as a natural mechanism exploited and controlled by cells to either produce variability or robustness in gene-expression programs, presumably in a context-specific way (Raj and van Oudenaarden, 2008). Transcriptional bursts are indeed modulated by external stimuli (Molina et al., 2013), by the developmental stage of the organism (Muramoto et al., 2012) and by chromatin state (Nicolas et al., 2018). However, we are still far from having a complete picture of how the delicate balance between robust control and variability in gene expression is achieved (Raj and van Oudenaarden, 2008).

Such balance is presumably gene and cell specific, and different for different biological processes. For example, the inflammatory response is characterized by a variable degree of transcriptional heterogeneity across genes, species and cell types (Hagai et al., 2018), whose connection to the dynamics of transcriptional bursting is unexplored. Transcription in inflammation depends on the dynamics of its master regulator

(Hayden and Ghosh, 2008): the transcription factor NF-κB. NF-κB dimers containing the monomer p65 (that we refer to as NF-κB in what follows) are activated by re-localizing from the cytoplasm to the nucleus upon inflammatory stimuli such as tumor necrosis factor alpha (TNF-α). This activation by nuclear localization is tightly regulated by a system of negative feedbacks (Hoffmann et al., 2002) so that cells display a variety of nuclear localization dynamics of NF-κB, including oscillations (Nelson et al., 2004; Tay et al., 2010; Zambrano et al., 2014a). Population-level measurements have shown that NF-κB dynamics lead to different dynamical patterns of mRNA expression (Ashall et al., 2009; Nelson et al., 2004; Sung et al., 2009; Zambrano et al., 2016). The NF-κB mediated nascent transcriptional response to stimuli at the population level is however fast, comparable with the translocation dynamics of NF-κB (Hao and Baltimore, 2013; Zambrano et al., 2016) that peaks at 30 min–1 h depending on the cell line and is accompanied by a fast binding of NF-κB to the promoter of target genes (Saccani et al., 2001).

Much less is known about how NF-κB dynamics modulates transcriptional variability at single cell level. Time-lapse analysis of NF-κB translocation, followed by analysis of mRNA expression at a single time-point through RNA FISH (Lee et al., 2014) and scRNA-seq (Lane et al., 2017) has demonstrated that different NF-κB dynamics translate into specific gene expression programs in single cells. Direct simultaneous observation of NF-κB dynamics and its gene expression products has so far been carried out at the protein level only, using GFP-transgenes (Nelson et al., 2004). More recent studies have begun to interrogate systematically how the NF-κB mediated transcriptional dynamics is modulated at the single-cell level by making use of a destabilized GFP transgene under the control of an HIV-LTR promoter (carrying two binding sites for NF-κB (Stroud et al., 2009)). In these studies, TNF-α induced gene expression has been shown to occur in bursts that are tuned by the insertion site of the transgene (Dar et al., 2012) and that are amplified by TAT-mediated positive feedbacks upon viral activation (Wong et al., 2018). However, as these assays are based on protein reporters with limited temporal resolution, the relationship between NF-κB nuclear localization and transcriptional dynamics at single cell level and its connection with the population level remains unexplored.

To address this, here we analyzed the cellular response to TNF-α at single-cell level in terms of NF-κB localization and nascent transcription, both for multiple genes in fixed cells (by single-molecule RNA FISH) and for a MS2 reporter gene controlled by an HIV-LTR promoter (Tantale et al., 2016) in living cells (by time-lapse imaging). We find that although different genes are expressed with different degrees of variability, they share common average population dynamics of nascent transcription that is *prompt* (i.e. occurs simultaneously with NF-κB translocation) and *sharp* (i.e. it is limited in time and decays faster than NF-κB nuclear localization). Live-cell analysis combined with repeated stimulation using microfluidics reveals that the population's sharp response is due to two factors: (i) a fraction of cells – first responders – that respond promptly and synchronously to TNF-α and are more prone to respond to multiple stimuli and (ii) a characteristic gene inactive time, during which the gene is insensitive to reactivation, following each active

period. Mathematical modelling shows that indeed only the combination of transcriptional activity driven by NF-κB localization and a gene activity module including a refractory state can recapitulate the promptness and the sharpness of the transcriptional response.

Our results show how the interaction of NF-κB localization dynamics and target gene activity can produce a timely and gene-specific collective response upon inflammatory stimuli.

Results

Population-level NF-κB-mediated transcription is prompt and sharp, despite being heterogeneous in single cells

To characterize transcriptional dynamics of inflammatory genes at single-cell level, HeLa cells were exposed to TNF-α and mature and nascent transcripts of three NF-κB target genes (*NFKBIA* coding for NF-κB main inhibitor IκBα, *IL6* for the cytokine IL6 and *TNF* for the cytokine TNF-α) (Rabani et al., 2011; Sung et al., 2009; Zambrano et al., 2016) were quantified at different timepoints (**Figure S1**) using single molecule fluorescence in-situ hybridization (Tsanov et al., 2016) (smFISH, see **Transparent Methods**). smFISH allows counting both nascent RNA molecules at active transcription sites (TS), which appear as 1 or 2 bright dots in the nucleus, and mature mRNA molecules, which appear as individual dots scattered in the nucleus and in the cytoplasm (**Figure 1A** and **Figure S2A**). In response to 10 ng/ml TNF-α, transcription of the three tested genes was induced with different degrees of cell-to-cell variability (**Figure 1A and 1B**). Such variability is captured by the Gini coefficient (Shaffer et al., 2017), a metric that ranges between 0 -when all cells express the same number of mRNAs- and 1 -when all mRNAs are detected in just one cell. *NFKBIA* displayed the most uniform expression (Gini ranging between 0.21 and 0.26, comparable to what previously reported for housekeeping genes (Shaffer et al., 2017)), while *IL6* (Gini from 0.41 to 0.55) and *TNF* (Gini from 0.29 to 0.33) were more unevenly expressed. Such different degrees of heterogeneity of the analyzed genes can be related to different bursting kinetics (Tunnacliffe and Chubb, 2020). By fitting the distribution of mature RNAs in single cells to a simple negative binomial model (Tunnacliffe and Chubb, 2020) whose parameters depend on the bursts' features (Raj et al., 2006) (**Figure S2B**) we estimate a higher relative burst frequency for *TNF* and *NFKBIA* than for *IL6*. The gene activity at single-cell level, estimated as the fractions of cells carrying active TS, indeed strongly differed among the genes considered: after stimulation *NFKBIA* TS were detectable in the largest fraction of cells (ranging from 84% at 20 min to 44% at 3h post TNF-α) followed by *IL6* TS (ranging from 32% to 21%) and *TNF* TS (from 16% to 9%) (**Figure 1C**).

Surprisingly, despite the observed heterogeneity in mRNA levels and active TS numbers at single cell level, the population average of the nascent transcriptional dynamics was remarkably similar for all genes, peaking at 20 min post stimulation as measured by either smFISH (**Figure 1D**) or intron-targeted qPCR (**Figure S2C** and **Transparent Methods**). Published models for NF-κB mediated gene expression suggest that RNAs are generated proportionally to NF-κB nuclear abundance (Lee et al., 2014; Zambrano et al., 2014b). We tested this notion by comparing nascent transcriptional dynamics with the abundance of nuclear NF-κB –a classical measure of NF-κB activation– obtained by immunofluorescence (see **Transparent Methods**) at different time points. Similar to previous reports (Lee et al., 2014), nuclear NF-κB accumulated rapidly and rather homogeneously across the cell population, peaking after 20 minutes and then decreasing in the following three hours (**Figure 1D and S2D**). Surprisingly, following its peak at 20 minutes, average nascent transcription

decreased faster than nuclear NF-κB abundance (**Figure 1D**): the time $t_{1/2}$ for the average nascent RNA signal to decrease to half of the peak value is ~30 min, whereas it is ~100 min for the average NF-κB nuclear localization (**Figure 1D**).

Taken together, our data show that the transcriptional activation of NF-κB target genes is gene- and cell-dependent. However, at population level their nascent transcription is *prompt*, since it peaks synchronously with NF-κB nuclear localization within our temporal resolution, and *sharp*, since it decays faster than NF-κB nuclear localization. We then decided to investigate further how these population-level features emerge from single-cell bursting dynamics using a live-cell reporter for nascent transcription.

A live-cell reporter of NF-κB-driven nascent transcription recapitulates the dynamics of endogenous genes

To monitor transcription induced by NF-κB in single living cells we used the HeLa 128xMS2 cell line (Tantale et al., 2016) (see **Transparent Methods**). Briefly, these cells harbor a single integration of a reporter gene containing 128 intronic repeats of the MS2-stem loop that are bound by a phage coat protein fused to GFP (MCP-GFP), such that bright spot within the nucleus denotes an active TS (**Figure 2A**). The reporter gene is under the control of the HIV-1 LTR, which contains two NF-κB binding sites (Stroud et al., 2009); this compares with the promoters of classic NF-κB targets, which typically harbor from 1 to 5 binding sites (Siggers et al., 2010). TNF-α stimulation induces transcription, as assessed by PCR after 1 hour of stimulation with 10 ng/ml TNF-α (**Figure S3A**). We visualized transcription in our cells using a sensitive widefield microscope (see **Transparent Methods**), which allows to visualize both the TS and the single molecules of released transcripts (RNAs, see **Transparent Methods** and insets of **Figures 2B-C**). Similar to what observed for *IL6* and *TNF*, we found active TS in only a relatively small fraction of cells (20%) 1 hr after TNF-α induction; an additional 20% of cells displayed mature RNAs but not active TS (**Figures 2C and 2D**). This fractional response was confirmed by smFISH using probes targeting the MS2 RNA (**Figure S3B**) and cannot be ascribed to reporter loss, since active TS were present in 10 out of 10 clonal sub-populations generated (**Figure S3C**)**.** Interestingly, as for the endogenous genes, a fraction of unstimulated cells (5%) also displayed active TSs while 20% displayed only released RNAs (**Figures 2B and 2D**), suggesting previous transcriptional activity potentially due to nonzero nuclear NF-κB basal levels or spontaneous activations, as reported (Zambrano et al., 2014a) – or to infrequent activation of our reporter by independent pathways. Importantly, the population average of MS2 nascent transcriptional dynamics is similar to that of the selected endogenous genes, and specifically displays a prompt and sharp response (**Figure S3D**). Hence, our MS2 reporter reproduces both single-cell and population-level features of endogenous NF-κB target genes and thus can be considered a faithful tool to study NF-κB regulated transcription.

NF-κB mediated transcriptional response is bursty and shaped by a population of "first responders"

We then used our reporter to characterize nascent transcriptional dynamics by monitoring the TS signal in single 128xMS2 cells over time, using a confocal microscope (**Figure 3A**, upper panels). We recorded 3D stacks of 10 μm depth every 3 minutes for 3 hours. A custom software allows to track the cell and detect the TS after a high pass filter of the stack maximal projection (see **Transparent Methods** and **Fig. S4A**). The maximum signal intensity of the TS is informative of the total TS intensity, since they correlate (see **Figure S4B**), while it is independent from the expression level of MCP-GFP in the cell (**Figure S4C**). The TS signal is then compared to the MCP-GFP background intensity to distinguish between transcriptionally "active" and "inactive" cells (see **Transparent Methods** and **Figure S4D**). Our time-lapse analyses showed that the MS2 transcriptional activity induced by TNF-α appears as discrete peaks, heterogeneous both in height and frequency, confirming experimentally the "bursty" feature that has been postulated from indirect measurements (Dar et al., 2012; Wong et al., 2018). In addition, "active" and "inactive" cells coexisted both after stimulation **Movie S1 and Fig. 3A**) or no stimulation (**Movie S2 and Fig. 3A**).

We repeated the time lapse imaging of our cells for different TNF-α doses and measured TS signals in hundreds of cells (**Figure 3B**). In color-plots, each line corresponds to a single TS observed for 180 minutes and the color reflects the TS signal intensity. The measured transcriptional response is strongly heterogeneous (**Movies S3 to S5**), but controlled by TNF-α, as the timing, the amplitude and the integrated intensity of the detected bursts are modulated by the dose (**Figure S5A**), as reported for bulk populations (Tay et al., 2010). Shear stress (Baeriswyl et al., 2019) potentially associated to plain addition of TNF-α-free medium does not lead to observable TS activity (**Figure S5B**).

Following previous work, we adapted the random telegraph model of transcription (Suter et al., 2011) to our MS2 reporter gene (**Figure 3C**) (see **Transparent Methods**) to determine the timespan of gene activations and estimate the evolution of the number of nascent transcripts in time, *n(t)*. The model accounts for the promoter switching between an active and an inactive state with rates k_{on} and k_{off}. Once the promoter is in its active state, new transcripts are generated with a rate equal to k^+ and processed/realeased with a rate equal to k^-. After verifying that the stochastic model could faithfully infer gene activation from synthetically generated TS time traces (**Figure S6A**), we fitted our experimental data with the model (**Figure 3C**) by imposing that the average number of nascent transcripts observed after 20 minutes of stimulation with TNF-α (10 ng/ml) would match with the average TS signal observed by smFISH (6 RNAs/cell). As the TS signal of our reporter can decrease in tens of transcripts per minute (Tantale et al., 2016), -the limited temporal resolution of our experiments does not allow to retrieve unique estimates for k^-, with multiple (k^+, k^-) pairs fitting the data equally well. Only the ratio of k^+ and k^- that determines the average burst amplitude could be determined. The behavior of the burst size is indeed informative:

in agreement with our previous analysis, the amplitude of the first burst is modulated by the dose of TNF-α (**Figure 3D**) and, more generally, the reporter transcriptional activity (estimated as AUC of *n(t)*) increases upon treatment with TNF-α (**Figure 3E**), due to an increase in the gene activation rate k_{on} and a decrease in the deactivation rate k_{off} (**Figure S6B**).

Importantly, we found a fraction of cells responding almost synchronously and within few minutes after TNF-α stimulation. This first response occurred earlier upon higher doses of TNF-α, as evinced by plotting the time t_{max} at which maximal TS activity was observed (**Figure 3F**). At 10ng/ml of TNF-α, the distribution of t_{max} was found to be bimodal (as evidenced by a change in the slope of the cumulative distribution, **Figure 3G**) allowing to identify a fraction of cells (approximately 40%) that respond within 30 minutes post-stimulation, that we define as 'first responders' (**Figure 3G**). Surprisingly, first responders display a stronger transcriptional activity than the other cells (**Figure 3H**), despite being indistinguishable from the rest of the cell population before stimulation with TNF-α (**Figure S6C**).

After this first burst of transcription, stochastic bursting dominates the individual cell response, as can be quantified by the evolution in time of the coefficient of variation of the number of nascent transcripts *n(t)*. The coefficient of variation has a minimum at 20 minutes (**Figure S6D**), which indicates an early synchronous round of transcription in a fraction of cells. The high synchronicity of bursting of these first responders at approximately 20 min post TNF-α lead to the observed prompt transcriptional response at population level.

First responders are more likely to respond strongly to consecutive pulses of TNF -α.

We next used our live-cell reporter to characterize to what extent cells are capable to respond to repeated stimulation. Using our previously described microfluidics setup (Zambrano et al., 2016) , we challenged our MS2x128 cells with two independent 1 hour pulses of 10 ng/ml TNF-α separated by a 2 hours washout (see **Transparent Methods**) and followed TS activity in hundreds of cells (**Figure 4A**). Similarly to what we observed for a single stimulation, the bursting parameters extracted from this two-pulses experiment were found to be modulated by TNF-α (**Figure S7A**). We then determined the fraction of cells responding to the first, to the second, and to both pulses (**Figure 4B** and **Movie S6**). A majority of responding cells responded to both pulses, and a fraction of cells responded to only one. Surprisingly, the fraction of cells responding to both pulses was significantly higher than what could be expected from statistically independent transcriptional activations (**Figure 4B** and **Transparent Methods**). Moreover, the maximum TS signal, expressed as number of nascent transcripts n_{max} for each pulse, was higher for cells responding to both TNF-α pulses than for cells responding to only either one of them (**Figure 4C**); the AUC behaves analogously (**Figure S7B**). Further, the timing to the maximum TS signal (t_{max}) after a TNF-α pulse was shorter on average

for cells that respond to both pulses than for cells that respond to just one (**Figure 4D**), and similar to the t_{max} of the previously identified "first responders".

Overall, our results suggest that despite an intrinsic variability in gene activation (cells can respond to either one TNF-α pulse or to both), there is a higher than expected proportion of cells that respond to both pulses, which excludes the statistical independence of the two responses. The data indicate that those cells are in a "first responder" state lasting longer than 180 minutes; first responders are activated faster, higher and more often than other cells.

The timing of the nascent transcriptional response does not depend on NF-κB nuclear localization dynamics at single-cell level

Once we established that the population-level transcriptional response to TNF-α is the result of heterogeneous transcriptional activation in single cells, we asked whether the latter emerged from heterogeneous nuclear localization dynamics of NF-κB. We stably transfected our MS2x128 cells with a previously validated RFP-p65 construct (Bosisio et al., 2006) (**Figure 5A**) and measured concomitantly TS signal intensity and NF-κB nuclear localization in single living cells (see **Transparent Methods**, **Figure 5A** and **Movie S7**). Although NF-κB nuclear localization dynamics varies across single responding cells (see **Transparent Methods**), as previously reported (Lee et al., 2014; Tay et al., 2010), we find that the nascent transcriptional response is even more heterogeneous (**Movies S8-S10**) as shown in previous experiments, and includes a fraction of "first responders". Parameters governing the bursting kinetics were found similar to those obtained from untransfected cells (**Figure S8A**), excluding an effect of transfection on results. At the single cell level, the fold change NF-κB nuclear abundance does not correlate with the peak value of nascent transcription nor its integrated value, neither when such correlations are evaluated for prompt responders (r^2<0.1 for all of them) (**Figure S8B-C**). This is somehow in contrast with reports showing a correlation between the fold change nuclear NF-κB and mature transcriptional output by smFISH (Lee et al., 2014; Wong et al., 2019). This discrepancy can have different experimental sources, the most evident one is that, differently from smFISH, our live-cell assay has no direct access to the amount of mature RNA released from the TS. Another possibility is that, since the ectopic (labeled) NF-κB is expressed heterogeneously across our population of transfected cells, the proportionality of the fold change of RFP- NF-κB and the endogenous one varies between cells and this blurs correlations. In any case, our data shows how a relatively uniform and synchronous nuclear translocation of NF-κB drives highly non-uniform transcription at single cell level, which highlights the apparent stochastic nature of the transcriptional activation process. Such stochasticity presumably arises as a combination of the intrinsic molecular noise of the transcriptional process and the concomitant action of other regulatory players alongside NF-κB, whose activity might further determine the transcriptional output.

Time-resolved measurements allowed us to quantify more finely the promptness of the transcriptional response. By superimposing the average data for NF-κB translocation and MS2 reporter transcriptional activity we found that both peak almost simultaneously at about 20 minutes post stimulation (both for transfected and untransfected cells, **Figure 5B**). Of note, ChIP-seq data on macrophage-like cells (Saccani et al., 2001) show a peak 20 min post-LPS stimulation in NF-κB binding to the promoter of a subset of certain NF-κB target genes, consistent with our observation for nascent transcription. The time at which NF-κB nuclear translocation peaks (typically the only peak, see **Figure S8D**) is relatively uniform compared to the first peak of nascent transcription (**Figure 5C**). Indeed the timing of the peak in NF-κB translocation matches on average that of the transcriptional response of the cells previously identified as "first responders"(**Figure 5C**), indicating that nuclear NF-κB might act at population level as a "limiting factor" for transcriptional activation of our reporter. This is compatible with the observation that NF-κB can find its targets rapidly (search time ~2 min), as can be derived from recent single molecule imaging data (Callegari et al., 2019) (see **Transparent Methods**). Of note, a small fraction of cells keeps transcribing even if NF-κB nuclear concentration has decreased (see e.g. **Movie S9**), which might reflect a population heterogeneity in NF-κB binding to the promoter, as indicated by other studies (Callegari et al., 2019). We also quantified the sharpness of the nascent transcriptional response and of NF-κB localization by computing their time $t_{1/2}$. The TS signal decayed faster than NF-κB nuclear abundance, in agreement with what observed for endogenous genes by smFISH. Thus, sharpness is reproduced faithfully by time-lapse imaging of our reporter gene (**Figure 5D**).

In short, these results illustrate how the nascent transcriptional response to TNF-α is more heterogeneous than NF-κB nuclear localization among the cells in the population. Moreover, we identify a fraction of first responder cells whose maximum transcriptional activity occurs simultaneously to NF-κB maximum nuclear translocation and is stronger than for the rest of the cells, so it is responsible for the prompt and sharp transcriptional response emerging at population level.

A model combining NF-κB mediated gene activation and a refractory state recapitulates the prompt and sharp nascent transcriptional response

To gain insights on the origin of the prompt and sharp NF-κB mediated transcriptional response, we explored mathematical models for NF-κB-driven transcription. We performed stochastic and deterministic simulations of gene activity (see **Transparent Methods**) and compared their results to our experimental data. A first candidate for our exploration was the random telegraph model of transcription, where the gene switches between on and off states in a purely stochastic fashion, with constant switching rates. This model however could not recapitulate our experimental data. For example, the experimentally measured gene off-times are

described by a unimodal distribution with a shape that varies between unstimulated and stimulated conditions (**Figure 6A**), rather than by the exponential that would be expected from the random telegraph model (Model 0, **Figure 6B**). Two alternative mechanism have been suggested to give rise to these unimodal distributions: a) the presence of a gene refractory state (Molina et al., 2013; Suter et al., 2011) that prevents the gene from immediately starting a second round of transcription after the first one is over and b) an oscillatory modulation of the gene activation (Zambrano et al., 2015). As shown below, the combination of these two features could reproduce the experimental features that we observed.

In previous explorations we simulated NF-κB response to TNF-α using a simple mathematical model (Zambrano et al., 2014b) (see **Figure 6B** and **Transparent Methods**); here, we analyzed the transcriptional dynamics of a prototypical target gene by modelling different NF-κB controlled gene activation-deactivation schemes inspired by experimental observations, among which our own. We used deterministic modeling to simulate population-average gene activity dynamics (**Figure S9A**) and stochastic modeling to simulate bursty stochastic transcription at single cell level, including the distribution of the off times (**Figure S9B**). The key parameters considered are the gene inactivation (k_{off}) and activation rates (k_{on}), which we varied four orders of magnitude around values used in the literature (Tay et al., 2010; Zambrano et al., 2014b) (see **Transparent Methods**). To constrain our exploration, we modeled first the gene activation rate as depending linearly (non-cooperatively) on NF-κB nuclear concentration, as proposed in a number of models (Tay et al., 2010; Zambrano et al., 2014b) and deduced from previous experiments and thermodynamic considerations (Siggers et al., 2010) (Model i, **Figure 6B**). This model allows to reproduce the non-monotonocity of the off times observed experimentally (**Figure 6B**), as predicted (Zambrano et al., 2015), but is unable to reproduce the prompt and sharp gene activation observed in our experiments (**Figure 6C**).

A recently proposed mechanism that in principle could rapidly shut down transcriptional activity and produce "sharpness" is molecular stripping, by which IκBα actively induces the dissociation of NF-κB from its binding sites on DNA (Dembinski et al., 2017; Potoyan et al., 2016) (Model ii, **Figure 6B**). A model based on molecular stripping reproduces the unimodal distribution of the inactivation times (**Figure 6B**) and we could indeed identify a sector of parameter space – low k_{on} and high k_{off} values – resulting in sharp transcriptional responses at the population level (**Figure 6B**). However, these parameters were not compatible with a prompt transcriptional activation, which was found for high k_{on} values instead (see purple areas in **Figure 6C** and examples in **Figure S9C**). To test these predictions, we co-treated our cells with TNF-α and cycloheximide (CHX), which blocks protein synthesis and hence IκBα synthesis and stripping. CHX is effective as demonstrated by the progressive decay observed in the nuclear fluorescence of MCP-GFP (**Movie S11**) and by higher NF-κB nuclear localization post TNF-stimulation (**Figure S9D**), as expected from blocking IκB re-synthesis. However, the decay time of the TS signal after reaching its maximum at t_{max} is almost unchanged by CHX, indicating that it does not depend on IκBα re-synthesis and stripping (**Figure S9E**).

Finally, we tested a model that combines the two previously mentioned mechanisms: NF-κB mediated activation by nuclear translocation and a gene refractory state (Model iii, **Figure 6B**). It is important to distinguish this gene refractory state from the "refractory state" in the NF-κB system arising due to feedback signaling (via the protein A20); the latter might preclude NF-κB response to consecutive TNF-α pulses (Adamson et al., 2016; Zhang et al., 2017). Here we do not explore how these two type of refractoriness might interact, an interaction that deserves future exploration. As previously reported (Molina et al., 2013), our model with a gene refractory state reproduces the non-monotonous distribution of "off times" of our bursty transcription data (**Figure 6B**). Interestingly, we find a wide region of parameter space (characterized by high k_{on} and k_{off}) compatible with both prompt and sharp gene activation (see green squared areas in **Figure 6C** and examples in **Figure S10A**). Furthermore, the simulated bursts have a structure clearly reminiscent of our experimental data, differently from the ones obtained from the other models (**Figure S10B**). Importantly, model iii is able to reproduce two key features: (i) the temporal evolution of the coefficient of variation of nascent transcription that we observed experimentally, with maximum synchronization of the bursts approximately 20 min post-stimulation (**Figure S10C**), and (ii) the presence of a fraction of first responders in the cell population (**Figure S10D)**. When using the experimentally determined NF-κB nuclear dynamics as input to simulate the gene activation rates of each single cell following the scheme of Model iii, we also reproduced a population-level prompt and sharp nascent transcriptional response (**Transparent Methods** and **Figure S10E**).

Hence, a gene refractory state is necessary to recapitulate the experimentally determined features of NF-κB mediated nascent transcription upon TNF-α, including a prompt and sharp transcriptional response emerging from a fraction of first responders.

Discussion

NF-κB dynamics is fundamental for the proper temporal development of inflammation. Previous reports (Ashall et al., 2009; Nelson et al., 2004; Sung et al., 2009) had shown that the NF-κB mediated transcriptional response to TNF-α can display a variety of dynamics, including genes whose mature transcripts peak early (at 30 min) or late (>3 hours), and even oscillating and non-oscillating gene expression patterns (Zambrano et al., 2016). We and others (Hao and Baltimore, 2013; Zambrano et al., 2016) suggested that such mRNA expression patterns arise from a common nascent transcriptional response, that peaks typically 20-30 minutes post stimulation. However, all these observations were based on population-level transcriptional measures, so how single-cell transcriptional response contributes to these features remained an open question that we have addressed in this work.

Different endogenous genes are expressed with different degrees of variability among individual cells upon TNF-α, but share a common population-level prompt and sharp nascent transcriptional response. Using single-cell smRNA-FISH for three bona-fide NF-κB target genes at different time points post TNF-α stimulation, we found that all of them were expressed heterogeneously across the population, although *NFKBIA* (coding for the inhibitor IκBα) was expressed more uniformly than *IL6* and *TNF*, coding for cytokines. Surprisingly, though, we found that the population dynamics of the nascent transcriptional response was very similar for these three genes, in spite of their marked differences in expression level and variability at single cell level, with Gini coefficients ranging from 0.2 to 0.5. Concomitant measurement of NF-κB nuclear localization by immunofluorescence showed that their common nascent transcriptional response is *prompt*, peaking simultaneously with NF-κB nuclear abundance, and *sharp*, decaying faster than the peak of NF-κB nuclear localization.

Population-level promptness and sharpness arises from heterogeneous bursting in single cells, including a fraction of "first responders". NF-κB response to TNF-α has been described as "digital", giving rise to a transcriptional output proportional to the fraction of cells displaying NF-κB translocation (Tay et al., 2010), which suggested a relatively uniform transcriptional response across those cells. Instead, using our MS2 nascent transcription reporter we find that a relatively uniform translocation of NF-κB in our cells (100% responding to 10 ng/ml of TNF-α, as assessed by immunofluorescence) gives rise to an extremely heterogeneous transcriptional response. This includes a fraction of "first responders", cells that reach a maximum transcriptional response higher and earlier than the other cells, and are more likely to respond to consecutive pulses of TNF-α. Interestingly, a fraction of "first responders" was identified when studying cellular responses to viral-activated interferon-beta signaling (Patil et al., 2015). smFISH data for endogenous genes *NFKBIA*, *IL6* and *TNF* also confirm a peak of TS activity for a fraction of cells within 20 minutes. We

ascribe the nascent transcriptional response at the population level to first responders that start transcribing earlier and more strongly than the other cells. Such rapid surge in nascent transcription is compatible with a short NF-κB search time on chromatin and transcriptional initiation can indeed occur nearly simultaneously to NF-κB translocation in the nucleus, as we observe experimentally in some cells.

The transcriptional response to consecutive TNF-α pulses has a stochastic component that is relevant to HIV latency. When challenging our cells with two pulses of TNF-α we find that while some cells respond to both pulses, some will respond just to the first or the second. Our cells harbor an LTR-HIV1 promoter, therefore this observation could represent the microscopic equivalent of a recently identified mechanism involved in HIV1 latency, where proviruses not induced after a first stimulation can be induced by a second one (Ho et al., 2013). This mechanism leads to a stochastic latency exit and it is clinically important as it may prevent curing patients from the virus by the "shock-and-kill" approach. In this context, it important to point out that negative feedback mediated by the IKK inhibitor A20 (a target of NF-κB) has also been shown to result in a fraction of cells where NF-κB does not respond to pulsatile stimulation with TNF-α (Adamson et al., 2016; Zhang et al., 2017). Such phenomenon is more evident for pulses separated by less than 100 minutes (Adamson et al., 2016) so presumably may be uncoupled from our observed behavior of the first responders, although the interaction between these different layers of regulation might be important for pulses in different timescales and deserves further exploration.

Analysis of transcriptional bursts highlights the existence of a characteristic inactive time after each gene activation. Our live cell imaging analysis of nascent transcription shows that after gene activations –during which multiple bursts of transcription can occur– there is typically a gene inactive time of approximately 25 minutes. This is characterized by a unimodal distribution of the gene "off" times obtained from our stochastic inference framework. Our previous theoretical work (Zambrano et al., 2015) and simulations presented here show that such characteristic unimodal distribution can in principle arise from NF-κB-driven gene activation in a gene that has just two states (2-states model). However, these 2-states models (where inactivation is either spontaneous or driven by the inhibitor IκBα through "molecular stripping" (Potoyan et al., 2016)) were unable to reproduce our key experimental findings of promptness and sharpness.

Only a mathematical model combining both NF-κB driven gene activation and a refractory state can reproduce experimental observations of promptness and sharpness. Unimodal distributions in the gene off times were also observed by others (Molina et al., 2013; Suter et al., 2011; Tantale et al., 2016) and modelled by adding an additional gene refractory state (3-states model). A study of our gene reporter under the control of HIV TAT protein suggested that a non-permissive state on the timescale of tens of minutes can be related to the dissociation of TBP from the promoter (Tantale et al., 2016). Here, by combining these 3-states model with NF-κB mediated activation and a gene refractory state, we could reproduce the experimentally observed dynamics of transcription: a unimodal distribution of off times and a prompt and sharp response at

population level. This model also reproduces other features in our experiments that 2-states models cannot, such as the existence of a fraction of "first responders" and a peak of bursting synchrony at 20 minutes post-stimulus. Overall, our model illustrates how a simple 3-states dynamics can produce a heterogeneous transcription activity at single-cell level and at the same time a sharp population-level transcriptional output. Further, our results confirm and reinforce recent theoretical modelling indicating that, counter-intuitively, gene refractory states can promote the rapid control of transcription in response to external stimuli (Li et al., 2018).

Sharp and prompt nascent transcriptional responses emerging from a fraction of "first responders": a general feature for inducible transcription factors? Previous population-level work on transcription suggested that gene-specific NF-κB driven expression profiles are mostly controlled by mRNA processing and degradation (Hao and Baltimore, 2013, 2009), while nascent transcription dynamics are shared among the different genes (Zambrano et al., 2016). Our work reinforces this viewpoint with a single-cell perspective, since we show how a uniform transcriptional dynamics emerge from prompt and bursty transcription in single cells. If mRNA degradation controls the temporal evolution of gene expression, a prompt and sharp peak of nascent transcription is a better-suited input to generate gene-dependent expression profiles as compared to a slowly varying transcriptional activity. The observed refractory state might have evolved from the necessity of sharpening the inherently stochastic transcriptional process, providing an opportunity window for decision (Zambrano et al., 2016). Furthermore, it is enough to provide a fraction of "first responders", which might be useful to temporally stratify the population response to stimuli. It also worth to speculate what molecular mechanisms could define the "first responder" state. In our analysis, we could not identify first responders depending on the pre-stimulus transcriptional activity or on the initial NF-κB nuclear concentration. Therefore, it is possible that for some cells the promoters of NF-κB dependent genes are primed in *cis*- to respond rapidly to the increase in NF-κB abundance, for example through higher accessibility or the pre-loading of poised polymerase. Of note, recent genome-wide analysis of NF-κB mediated nascent transcription in mouse embryonic fibroblasts revealed a class of very early genes (including *TNF*), with nascent transcripts peaking as early as 15 min post stimulation (Ngo et al., 2020) – earlier than the peak in NF-κB nuclear concentration. Detailed ChIP analysis at the promoters of these genes might therefore shed light on the nature of first responders.

Prompt and sharp transcriptional profiles are observed for other inducible transcriptional programs, ranging from stress response to nutrient detection and development (Hafner et al., 2020; Senecal et al., 2014; Stevense et al., 2010). Further, other inducible transcription factors such as p53 have similar search times (Loffreda et al., 2017) to the one we calculated for NF-κB and produce population-level gene-independent nascent transcription dynamics and gene-specific mRNA profiles due to differential RNA degradation (Hafner et al., 2017; Koh et al., 2019; Porter et al., 2016). It is then tempting to speculate that other transcription

factors that need to respond rapidly to intracellular (e.g. p53) (Hafner et al., 2017) or extracellular cues (e.g. c-FOS, STAT3, GR) (Alonzi et al., 2001; Stavreva et al., 2019) might exploit a similar design principle to produce a time-resolved, prompt and sharp nascent transcriptional response.

In conclusion, our data and models show how the expression of NF-κB target genes can be coordinated at cell population level and yet be heterogeneous across single cells, and further provide a framework for understanding how transcription factors can achieve prompt and sharp transcriptional responses.

Limitations of study

This study is focused on the transcriptional response of HeLa cells to TNF-α; the behavior of nascent transcription for other cells–including primary cells- might vary from what we report here. We find a population-level prompt and sharp response to TNF-α in a panel of representative NF-κB targets and in an MS2 reporter driven by NF-κB, however we cannot exclude other NF-κB controlled genes might show a different dynamics of the nascent transcriptional response. Finally, to find the precise relation between NF-κB nuclear abundance and nascent transcriptional output at single-cell level it would be necessary to fluorescently tag the endogenous p65; our use of an ectopic tagged p65 only allows us to establish a qualitative – population level - relationship between nascent transcriptional dynamics and NF-κB nuclear localization dynamics.

Resource Availability

Lead Contact

The lead contact for this study is Samuel Zambrano (zambrano.samuel@hsr.it).

Materials Availability

All unique reagents generated in this study are available from the corresponding authors with a completed Material Transfer Agreement.

Data and Code Availability

The stochastic simulation and inference software is available at: https://github.com/MolinaLab-IGBMC/. Software for deterministic simulations and quantification of transcription in our MS2 system can be found at: https://github.com/SZambranoS/.

Acknowledgements

We are grateful to F. Mueller (Institut Pasteur, Paris) for help with the smiFISH protocols. The research leading to these results has received funding from Fondazione Cariplo (A.L. and D.M.: 2014-1157 to D.M.), OSR (OSR Seed Grants to S.Z. and D.M.) and the Italian Cancer Research Association (AIRC, D.M. IG 2018-21897, A.A., F.C., E.C. and S.Z. IG 2017-18687 to A. A.).

Author contribution

Conceptualization: SZ, NM, DM

Supervision: SZ, AA, MEB, CT, DM

Visualization: SZ, AL, NM, DM

Formal Analysis: SZ, AL, AA, MEB, NM, DM

Investigation: SZ, AL, EC, GS, FC, EB, NM, DM

Writing-Original draft: SZ, DM

Writing-review and editing: SZ, EB, CT, AA, MEB, NM, DM

Funding acquisition: SZ, CT, EB, AA, MEB, DM

Declaration of Interests

The authors declare no competing interests

References

Adamson, A., Boddington, C., Downton, P., Rowe, W., Bagnall, J., Lam, C., Maya-Mendoza, A., Schmidt, L., Harper, C.V., Spiller, D.G., Rand, D.A., Jackson, D.A., White, M.R.H., Paszek, P., 2016. Signal transduction controls heterogeneous NF-κB dynamics and target gene expression through cytokine-specific refractory states. Nat Commun 7. https://doi.org/10.1038/ncomms12057

A.Hoffmann, Levchencko, A., Scott, M.L., Baltimore, D., 2002. The IkappaB-NF-kappaB signalling module: temporal control and selective gene activation. Science 298, 1241–1245.

Alonzi, T., Maritano, D., Gorgoni, B., Rizzuto, G., Libert, C., Poli, V., 2001. Essential Role of STAT3 in the Control of the Acute-Phase Response as Revealed by Inducible Gene Activation in the Liver. Molecular and Cellular Biology 21, 1621–1632. https://doi.org/10.1128/MCB.21.5.1621-1632.2001

Ashall, L., Horton, C.A., Nelson, D.E., Paszek, P., Harper, C.V., Sillitoe, K., Ryan, S., Spiller, D.G., Unitt, J.F., Broomhead, D.S., Kell, D.B., Rand, D.A., See, V., White, M.R.H., 2009. Pulsatile Stimulation Determines Timing and Specificity of NF- B-Dependent Transcription. Science 324, 242–246. https://doi.org/10.1126/science.1164860

Baeriswyl, D.C., Prionisti, I., Peach, T., Tsolkas, G., Chooi, K.Y., Vardakis, J., Morel, S., Diagbouga, M.R., Bijlenga, P., Cuhlmann, S., Evans, P., Kwak, B.R., Ventikos, Y., Krams, R., 2019. Disturbed flow induces a sustained, stochastic NF-κB activation which may support intracranial aneurysm growth in vivo. Sci Rep 9, 1–14. https://doi.org/10.1038/s41598-019-40959-y

Bosisio, D., Marazzi, I., Agresti, A., Shimizu, N., Bianchi, M.E., Natoli, G., 2006. A hyper-dynamic equilibrium between promoter-bound and nucleoplasmic dimers controls NF-κB-dependent gene activity. The EMBO Journal 25, 798–810. https://doi.org/10.1038/sj.emboj.7600977

Callegari, A., Sieben, C., Benke, A., Suter, D.M., Fierz, B., Mazza, D., Manley, S., 2019. Single-molecule dynamics and genome-wide transcriptomics reveal that NF-kB (p65)-DNA binding times can be decoupled from transcriptional activation. PLoS Genet. 15, e1007891. https://doi.org/10.1371/journal.pgen.1007891

Chong, S., Chen, C., Ge, H., Xie, X.S., 2014. Mechanism of Transcriptional Bursting in Bacteria. Cell 158, 314–326. https://doi.org/10.1016/j.cell.2014.05.038

Dar, R.D., Razooky, B.S., Singh, A., Trimeloni, T.V., McCollum, J.M., Cox, C.D., Simpson, M.L., Weinberger, L.S., 2012. Transcriptional burst frequency and burst size are equally modulated across the human genome. Proc Natl Acad Sci U S A 109, 17454–17459. https://doi.org/10.1073/pnas.1213530109

Dembinski, H.E., Wismer, K., Vargas, J.D., Suryawanshi, G.W., Kern, N., Kroon, G., Dyson, H.J., Hoffmann, A., Komives, E.A., 2017. Functional importance of stripping in NFκB signaling revealed by a stripping-impaired IκBα mutant. PNAS 114, 1916–1921. https://doi.org/10.1073/pnas.1610192114

Elowitz, M.B., Levine, A.J., Siggia, E.D., Swain, P.S., 2002. Stochastic gene expression in a single cell. Science 297, 1183–1186.

Golding, I., Paulsson, J., Zawilski, S.M., Cox, E.C., 2005. Real-Time Kinetics of Gene Activity in Individual Bacteria. Cell 123, 1025–1036. https://doi.org/10.1016/j.cell.2005.09.031

Hafner, A., Reyes, J., Stewart-Ornstein, J., Tsabar, M., Jambhekar, A., Lahav, G., 2020. Quantifying the Central Dogma in the p53 Pathway in Live Single Cells. Cell Systems 10, 495-505.e4. https://doi.org/10.1016/j.cels.2020.05.001

Hafner, A., Stewart-Ornstein, J., Purvis, J.E., Forrester, W.C., Bulyk, M.L., Lahav, G., 2017. p53 pulses lead to distinct patterns of gene expression albeit similar DNA binding dynamics. Nat Struct Mol Biol 24, 840–847. https://doi.org/10.1038/nsmb.3452

Hagai, T., Chen, X., Miragaia, R.J., Rostom, R., Gomes, T., Kunowska, N., Henriksson, J., Park, J.-E., Proserpio, V., Donati, G., Bossini-Castillo, L., Vieira Braga, F.A., Naamati, G., Fletcher, J., Stephenson, E., Vegh, P., Trynka, G., Kondova, I., Dennis, M., Haniffa, M., Nourmohammad, A., Lässig, M., Teichmann, S.A., 2018. Gene expression variability across cells and species shapes innate immunity. Nature 563, 197–202. https://doi.org/10.1038/s41586-018-0657-2

Hao, S., Baltimore, D., 2013. RNA splicing regulates the temporal order of TNF-induced gene expression. PNAS 110, 11934–11939. https://doi.org/10.1073/pnas.1309990110

Hao, S., Baltimore, D., 2009. The stability of mRNA influences the temporal order of the induction of genes encoding inflammatory molecules. Nat. Immunol. 10, 281–288. https://doi.org/10.1038/ni.1699

Hayden, M.S., Ghosh, S., 2008. Shared Principles in NF-kappaB Signaling. Cell 132, 344–344.

Ho, Y.-C., Shan, L., Hosmane, N.N., Wang, J., Laskey, S.B., Rosenbloom, D.I.S., Lai, J., Blankson, J.N., Siliciano, J.D., Siliciano, R.F., 2013. Replication-competent non-induced proviruses in the latent reservoir increase barrier to HIV-1 cure. Cell 155, 540–551. https://doi.org/10.1016/j.cell.2013.09.020

Ko, M.S., Nakauchi, H., Takahashi, N., 1990. The dose dependence of glucocorticoid-inducible gene expression results from changes in the number of transcriptionally active templates. EMBO J 9, 2835–2842.

Koh, W.S., Porter, J.R., Batchelor, E., 2019. Tuning of mRNA stability through altering 3'-UTR sequences generates distinct output expression in a synthetic circuit driven by p53 oscillations. Scientific Reports 9, 1–8. https://doi.org/10.1038/s41598-019-42509-y

Lane, K., Valen, D.V., DeFelice, M.M., Macklin, D.N., Kudo, T., Jaimovich, A., Carr, A., Meyer, T., Pe'er, D., Boutet, S.C., Covert, M.W., 2017. Measuring Signaling and RNA-Seq in the Same Cell Links Gene Expression to Dynamic Patterns of NF-κB Activation. cels 4, 458-469.e5. https://doi.org/10.1016/j.cels.2017.03.010

Lee, R.E., Walker, S.R., Savery, K., Frank, D.A., Gaudet, S., 2014. Fold change of nuclear NF-kappaB determines TNF-induced transcription in single cells. Mol Cell 53, 867–879.

Li, C., Cesbron, F., Oehler, M., Brunner, M., Höfer, T., 2018. Frequency Modulation of Transcriptional Bursting Enables Sensitive and Rapid Gene Regulation. cels 6, 409-423.e11. https://doi.org/10.1016/j.cels.2018.01.012

Loffreda, A., Jacchetti, E., Antunes, S., Rainone, P., Daniele, T., Morisaki, T., Bianchi, M.E., Tacchetti, C., Mazza, D., 2017. Live-cell p53 single-molecule binding is modulated by C-terminal acetylation and correlates with transcriptional activity. Nat Commun 8, 313. https://doi.org/10.1038/s41467-017-00398-7

Molina, N., Suter, D.M., Cannavo, R., Zoller, B., Gotic, I., Naef, F., 2013. Stimulus-induced modulation of transcriptional bursting in a single mammalian gene. PNAS 110, 20563–20568.

Muramoto, T., Cannon, D., Gierliński, M., Corrigan, A., Barton, G.J., Chubb, J.R., 2012. Live imaging of nascent RNA dynamics reveals distinct types of transcriptional pulse regulation. PNAS 109, 7350–7355. https://doi.org/10.1073/pnas.1117603109

Nelson, D.E., Ihekwaba, A.E., Elliott, M., Johnson, J.R., Gibney, C.A., Foreman, B.E., Nelson, G., See, V., Horton, C.A., Spiller, D.G., Edwards, S.W., McDowell, H.P., Unitt, J.F., Sullivan, E., Grimley, R., Benson, N., Broomhead, D., Kell, D.B., White, M.R., 2004. Oscillations in NF-kappaB signaling control the dynamics of gene expression. Science 306, 704–708.

Ngo, K.A., Kishimoto, K., Davis-Turak, J., Pimplaskar, A., Cheng, Z., Spreafico, R., Chen, E.Y., Tam, A., Ghosh, G., Mitchell, S., Hoffmann, A., 2020. Dissecting the Regulatory Strategies of NF-κB RelA Target Genes in the Inflammatory Response Reveals Differential Transactivation Logics. Cell Reports 30, 2758-2775.e6. https://doi.org/10.1016/j.celrep.2020.01.108

Nicolas, D., Zoller, B., Suter, D.M., Naef, F., 2018. Modulation of transcriptional burst frequency by histone acetylation. PNAS 115, 7153–7158. https://doi.org/10.1073/pnas.1722330115

Patil, S., Fribourg, M., Ge, Y., Batish, M., Tyagi, S., Hayot, F., Sealfon, S.C., 2015. Single-cell analysis shows that paracrine signaling by first responder cells shapes the interferon-β response to viral infection. Sci Signal 8, ra16. https://doi.org/10.1126/scisignal.2005728

Pichon, X., Lagha, M., Mueller, F., Bertrand, E., 2018. A Growing Toolbox to Image Gene Expression in Single Cells: Sensitive Approaches for Demanding Challenges. Mol. Cell 71, 468–480. https://doi.org/10.1016/j.molcel.2018.07.022

Porter, J.R., Fisher, B.E., Batchelor, E., 2016. P53 Pulses Diversify Target Gene Expression Dynamics in an mRNA Half-Life-Dependent Manner and Delineate Co-regulated Target Gene Subnetworks. Cell Systems 2, 272–282. https://doi.org/10.1016/j.cels.2016.03.006

Potoyan, D.A., Zheng, W., Komives, E.A., Wolynes, P.G., 2016. Molecular stripping in the NF-κB/IκB/DNA genetic regulatory network. PNAS 113, 110–115. https://doi.org/10.1073/pnas.1520483112

Rabani, M., Levin, J.Z., Fan, L., Adiconis, X., Raychowdhury, R., Garber, M., Gnirke, A., Nusbaum, C., Hacohen, N., Friedman, N., Amit, I., Regev, A., 2011. Metabolic labeling of RNA uncovers principles of RNA production and degradation dynamics in mammalian cells. Nature Biotechnology 29, 436–442. https://doi.org/10.1038/nbt.1861

Raj, A., Peskin, C.S., Tranchina, D., Vargas, D.Y., Tyagi, S., 2006. Stochastic mRNA synthesis in mammalian cells. PLoS Biology 4, e309–e309.

Raj, A., van Oudenaarden, A., 2008. Nature, nurture, or chance: stochastic gene expression and its consequences. Cell 135, 216–226. https://doi.org/10.1016/j.cell.2008.09.050

Saccani, S., Pantano, S., Natoli, G., 2001. Two Waves of Nuclear Factor κb Recruitment to Target Promoters. J Exp Med 193, 1351–1360.

Senecal, A., Munsky, B., Proux, F., Ly, N., Braye, F.E., Zimmer, C., Mueller, F., Darzacq, X., 2014. Transcription factors modulate c-Fos transcriptional bursts. Cell Rep 8, 75–83. https://doi.org/10.1016/j.celrep.2014.05.053

Shaffer, S.M., Dunagin, M.C., Torborg, S.R., Torre, E.A., Emert, B., Krepler, C., Beqiri, M., Sproesser, K., Brafford, P.A., Xiao, M., Eggan, E., Anastopoulos, I.N., Vargas-Garcia, C.A., Singh, A., Nathanson, K.L., Herlyn, M., Raj, A., 2017. Rare cell variability and drug-induced reprogramming as a mode of cancer drug resistance. Nature 546, 431–435. https://doi.org/10.1038/nature22794

Siggers, L.G.T., Tiana, G., Caprara, G., Notarbartolo, S., Corona, T., Pasparakis, M., Milani, P., Bulyk, M.L., Natoli, G., 2010. Noncooperative interactions between transcription factors and clustered DNA binding sites enable graded transcriptional responses to environmental inputs. Mol. Cell 37, 418–428.

Stavreva, D.A., Garcia, D.A., Fettweis, G., Gudla, P.R., Zaki, G.F., Soni, V., McGowan, A., Williams, G., Huynh, A., Palangat, M., Schiltz, R.L., Johnson, T.A., Presman, D.M., Ferguson, M.L., Pegoraro, G., Upadhyaya, A., Hager, G.L., 2019. Transcriptional Bursting and Co-bursting Regulation by Steroid Hormone Release Pattern and Transcription Factor Mobility. Molecular Cell 75, 1161-1177.e11. https://doi.org/10.1016/j.molcel.2019.06.042

Stevense, M., Muramoto, T., Müller, I., Chubb, J.R., 2010. Digital nature of the immediate-early transcriptional response. Development 137, 579–584. https://doi.org/10.1242/dev.043836

Stroud, J.C., Oltman, A., Han, A., Bates, D.L., Chen, L., 2009. Structural basis of HIV-1 activation by NF-kappaB--a higher-order complex of p50:RelA bound to the HIV-1 LTR. J. Mol. Biol. 393, 98–112. https://doi.org/10.1016/j.jmb.2009.08.023

Sung, M.H., Salvatore, L., Lorenzi, R.D., Indrawan, A., Pasparakis, M., Hager, G.L., Bianchi, M.E., Agresti, A., 2009. Sustained Oscillations of NF-kappaB Produce Distinct Genome Scanning and Gene Expression Profiles. PLoS ONE 5, e7163–e7163.

Suter, D.M., Molina, N., Gatfield, D., Schneider, K., Schibler, U., Naef, F., 2011. Mammalian Genes Are Transcribed with Widely Different Bursting Kinetics. Science 332, 472–474. https://doi.org/10.1126/science.1198817

Tantale, K., Mueller, F., Kozulic-Pirher, A., Lesne, A., Victor, J.-M., Robert, M.-C., Capozi, S., Chouaib, R., Bäcker, V., Mateos-Langerak, J., Darzacq, X., Zimmer, C., Basyuk, E., Bertrand, E., 2016. A single-molecule view of transcription reveals convoys of RNA polymerases and multi-scale bursting. Nature Communications 7, 12248. https://doi.org/10.1038/ncomms12248

Tay, S., Hughey, J.J., Lee, T.K., Lipniacki, T., Quake, S.R., Covert, M.W., 2010. Single-cell NF-kappaB dynamics reveal digital activation and analogue information processing. Nature 466, 267–271.

Tsanov, N., Samacoits, A., Chouaib, R., Traboulsi, A.-M., Gostan, T., Weber, C., Zimmer, C., Zibara, K., Walter, T., Peter, M., Bertrand, E., Mueller, F., 2016. smiFISH and FISH-quant - a flexible single RNA detection approach with super-resolution capability. Nucleic Acids Res. 44, e165. https://doi.org/10.1093/nar/gkw784

Tunnacliffe, E., Chubb, J.R., 2020. What Is a Transcriptional Burst? Trends in Genetics. https://doi.org/10.1016/j.tig.2020.01.003

Wong, V.C., Bass, V.L., Bullock, M.E., Chavali, A.K., Lee, R.E.C., Mothes, W., Gaudet, S., Miller-Jensen, K., 2018. NF-κB-Chromatin Interactions Drive Diverse Phenotypes by Modulating Transcriptional Noise. Cell Reports 22, 585–599. https://doi.org/10.1016/j.celrep.2017.12.080

Wong, V.C., Mathew, S., Ramji, R., Gaudet, S., Miller-Jensen, K., 2019. Fold-Change Detection of NF-κB at Target Genes with Different Transcript Outputs. Biophys J 116, 709–724. https://doi.org/10.1016/j.bpj.2019.01.011

Zambrano, S., Bianchi, M.E., Agresti, A., 2014a. High-throughput analysis of NF-κB dynamics in single cells reveals basal nuclear localization of NF-κB and spontaneous activation of oscillations. PLoS ONE 9. https://doi.org/10.1371/journal.pone.0090104

Zambrano, S., Bianchi, M.E., Agresti, A., 2014b. A simple model of NF-κB dynamics reproduces experimental observations. J. Theor. Biol. 347C, 44–53. https://doi.org/10.1016/j.jtbi.2014.01.015

Zambrano, S., Bianchi, M.E., Agresti, A., Molina, N., 2015. Interplay between stochasticity and negative feedback leads to pulsed dynamics and distinct gene activity patterns. Phys Rev E Stat Nonlin Soft Matter Phys 92, 022711. https://doi.org/10.1103/PhysRevE.92.022711

Zambrano, S., de Toma, I., Piffer, A., Bianchi, M.E., Agresti, A., 2016. NF-kappaB oscillations translate into functionally related patterns of gene expression. eLife 5, e09100–e09100.

Zhang, Q., Gupta, S., Schipper, D.L., Kowalczyk, G.J., Mancini, A.E., Faeder, J.R., Lee, R.E.C., 2017. NF-κB dynamics discriminate between TNF doses in single cells. Cell Syst 5, 638-645.e5. https://doi.org/10.1016/j.cels.2017.10.011

Figure legends

Figure 1. Nascent transcription of NF-κB target genes is prompt and sharp. A. Exemplary smFISH acquisitions using probes targeting *NFKBIA, IL6* and *TNF* RNAs 20 min after induction with TNF-α. Maximum projection, scale bar 10 μm. **B.** Mature *MS2* transcripts per cell measured at different times following TNF-α. Also displayed is the Gini coefficient measured at 20', 1 hour and 3 hour after stimulation, as an estimate of the heterogeneity in the cell-by-cell expression of the three targets (n_{cells} =219, 270, 250, 206 for 0', 20', 1 hour, 3 hours; *IL6*: n_{cells} =187, 193, 220, 220 for 0', 20', 1 hour, 3 hours; *TNF*: n_{cells} =117, 90, 157, 140 Kruskal-Wallis test (KW), * p<0.05, ** p< 0.01, *** p<0.001, **** p<0.0001). **C.** Fraction of cells with either 0,1,2 or >2 active transcription sites for MS2 measured by smFISH (n_{cells}, statistical tests and p-value thresholds as in Figure 1B). **D.** Average number of nascent transcripts per cell measured by smFISH (black, error bars: SEM. n_{cells}, as in Figure 1B-C, KW test – not shown - provides the same pair-wise p-values as in Figure 1C) and normalized nuclear- NF-κB fluorescence intensity. The transcriptional peak is prompt, as it is almost simultaneous to that of NF-κB nuclear localization within our temporal resolution, and sharp, since it is sharper than the peak of NF-κB nuclear localization, as evaluated by linear interpolation as the time $t_{1/2}$ between maximal activation, $\max(A)$, and $0.5 \times \max(A)$ (indicated by a dashed line) (right panel, error bars calculated by computing the minimal and maximal slope of the lines passing through the 20' and 1h time-points). See also **Fig. S1-2** and **Table S1**.

Figure 2. Probing NF-κB transcription in single cells using a MS2 reporter. A. The MS2 reporter of TNF-α induced transcriptional activity. 128 MS2 stem loops RNAs are transcribed by the gene under the control of the NF-κB controlled LTR-HIV1 promoter, RNAs are bound by constitutively expressed MCP-GFP protein. As a result, a bright spot appears in the cell nuclei. **B.** Representative image of unstimulated cells observed with a high illumination microscope, allowing to observe cells with a visible active TS (inset, red frame), cells with single RNAs but no visible active TSs (inset, green frame) and none observed (inset, blue frame). **C.** Same for stimulated with 10 ng/ml of TNF-α. **D.** Quantification of the fraction of cells with visible RNAs and visible TSs show statistical difference between TNF treatment or no treatment (mean and SD of 2 independent experiments is plotted, t-test). See also **Fig S.3.**

Figure 3. Live cell imaging of MS2 reporter for different doses and stochastic modeling highlights a dose-dependent bursting behavior and the existence of a fraction of first responders to TNF-α. A. Exemplary images of a cell stimulated with 10 ng/ml TNF-α and acquired with our live cell imaging setup (maximum projection, scale bar 10 μm). Arrows indicate the detected TS signal. Tracks show TS signal for unstimulated and stimulated cells, either displaying bursts (green) and no bursts (red). Transcribing TS are identified by having signal above or below the threshold (dashed black line) established as four times the standard deviation of the background signals. **B.** TS signal for hundreds of cells, either unstimulated or stimulated with 1 or 10 ng/ml TNF-α, sorted for increasing TS signal. **C.** Scheme of the simple mathematical model of nascent

transcription *n(t)* with the activation and inactivation rates of the gene (k_{on} and k_{off}), the RNA accumulation rate (k^+) and the RNA release rate (k^-). Example of the inferred transcript levels *n(t)* from a time series of TS signal. **D.** Transcriptional activity during the first burst, and **E**. Transcriptional activity during the whole time course inferred as area under the curve (AUC) of *n(t),* for the three doses of TNF. **F.** Distribution of the timing of the maximum TS signal t_{max}, that decrease with the TNF-α dose . **G.** The cumulative distribution of t_{max} for the cells treated with 10ng/ml allows defining the fraction of cells as first responders, as those with t_{max} < 30 min. **H.** The peak transcriptional activity n_{max} is higher in first responders. In all panel, statistical significance is calculated with pairwise Kolmogorov-Smirnov tests. See also **Fig. S4-S6**.

Figure 4. Pulsed TNF-α stimulation shows that transcriptional bursts are not purely stochastic. A. TS signal for hundreds of cells for after two pulses of one hour of 10 ng/ml TNF-α separated by a two hours washout, sorted for increasing TS signal. Cells are clustered as non-responding – within 90 minutes of each pulse– responding to only one of the two pulses or responding to both pulses. **B.** Fraction of cells responding to none of the TNF-α pulses, just the first or just the second (mean and standard deviation of 3 independent experiments), and predicted fraction for statistically independent activation (random). **C.** Maximum TS signal (in number of transcripts) after the first and second pulse for the sub-populations identified above. Cells responding to both TNF–α pulses display a stronger response to both the first and the second pulse. **D.** The timing of the maximum of the TS signal after each TNF-α pulse, indicating that cells that are primed to response do so more quickly upon the first pulse that the remaining populations, in particular those responding only to the first or the second. See also **Fig. S7.**

Figure 5. Simultaneous imaging of NF-κB translocation and MS2 transcriptional activity highlights the promptness and sharpness of the transcriptional response. A. Top: exemplary images of cells stimulated with 10 ng/ml TNF-α before and after 30 minutes stimulation with 10 ng/ml TNF-α. Note the activation of NF-κB in all the cells, while the TS appears active in the indicated ones (arrows) at that specific time point. Bottom: TS signal activity and nuclear NF-κB activation for hundreds of cells sorted for increasing TS signal. **B.** Plot of the normalized average TS signal for three experiments of (green, standard deviation is represented), superimposed with the average NF-κB nuclear intensity assessed by live cell imaging (red) with standard deviation inferred from imaging data. The dark green line represents the TS activity of transfected cells, within the range of variability observed for untransfected cells. The plot indicates that both signals peak simultaneously but TS activation decrease more sharply. **C.** The quantification of the timing of the first maximum of NF-kB nuclear localization and of TS activity, showing that the medians are similar but the latter is more heterogeneous with prompt and late responders. **D.** Estimation of the variability of the decay time $t_{1/2}$ for the TS signal and NF-κB nuclear localization, obtained from panel B**.** The decay time of the transcription signal is much lower than that of NF-κB, indicating a sharper response. See also **Fig S8**

Figure 6. Identification of a minimal mathematical model recapitulating NF-κB mediated transcription dynamics. A. Example of the inferred transcript levels *n(t)* given a TS signal time series. The off times t_{off} are computed as described (top)**.** Unimodal distribution of the off times obtained from our experimental data (bottom). **B.** Scheme of a simple mathematical model where gene activation is modulated by NF-κB while inactivation is governed by the concentration of the inhibitor IκBα. Different possible mechanisms of activation of the target gene are considered. The classical telegraph model of transcription (Model 0) with constant activation and inactivation rates gives rise to exponential distribution of the off times (inset) so cannot describe experimental data. Based on the literature and our observation we propose alternative models: linear activation (Model i), molecular stripping (Model ii) and gene with a refractory state (Model iii). All of them reproduce the unimodal distribution of t_{off} (insets). **C.** We screened the timing of the peak of the gene activity (top panels) and the sharpness (bottom panels) of the peak for Models i to iii, two orders of magnitude above and below reference values ($k_{on,0}$ and $k_{off,0}$). The color-code indicates the promptness and the sharpness of the peak, respectively, as compared to the peak of nuclear NF-κB. Model i does not give prompt and sharp responses. Model ii gives prompt responses in a region that does not overlap with the region giving a sharp response, both highlighted with a purple square. Finally, Model iii with NF-κB mediated activation and a refractory state is the only one giving parameters combination (high k_{on} and k_{off}) leading to a prompt and sharp transcriptional response, highlighted with a green square. See also **Fig. S9-S10.**

Supplemental Movie Legends

Movie S1, related to Figure 3. Exemplary time-lapse acquisition for cells treated with 10ng/ml TNF-α. Shown are maximal projections.

Movie S2, related to Figure 3 Exemplary time-lapse acquisition for untreated cells. Shown are maximal projections.

Movie S3, related to Figure 3. Exemplary single-cell analysis of the MS2 signal intensity in a single cell upon treatment with 10ng/ml. The displayed cell shows a prompt response in minutes upon stimulation.

Movie S4, related to Figure 3. Exemplary single-cell analysis of the MS2 signal intensity in a single cell upon treatment with 10ng/ml. The displayed cell shows a late response.

Movie S5, related to Figure 3. Exemplary single-cell analysis of the MS2 signal intensity in a single cell upon treatment with 10ng/ml. The displayed cell shows no response.

Movie S6, related to Figure 4. Exemplary time-lapse acquisition for cells treated with two pulses of 10ng/ml TNF-α as described in figure 4. Shown are maximal projections.

Movie S7, related to Figure 5. Exemplary simultaneous acquisition of NF-kB translocation (left) and MS2 transcription dynamics (center, maximum projection shown). The overlay of the two channels is also shown.

Movies S8-S10, related to Figure 5. Exemplary single-cell analysis of the MS2 signal intensity (left, displayed in green in the plot) and NF-kB translocation (center, displayed in red in the plot) in single cells upon treatment with 10ng/ml.

Movie S11, related to Figure 6. Exemplary time-lapse acquisition for cells treated with TNF-α+CHX. Shown are maximal projections.

Figure 1

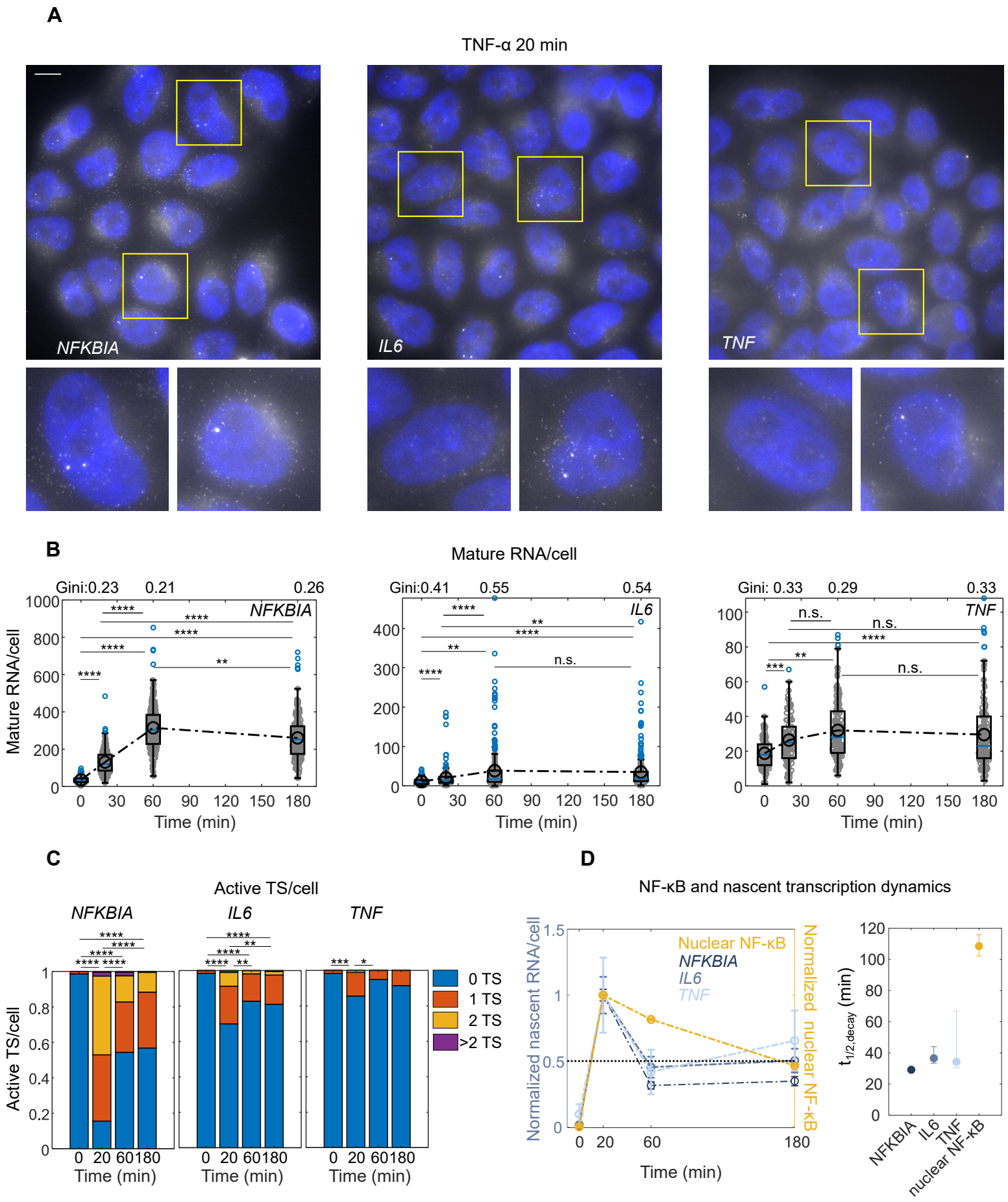
A
TNF-α 20 min
NFKBIA
IL6
TNF
B
Mature RNA/cell
Gini:0.23
0.21
0.26
Gini:0.41
0.55
0.54
Gini: 0.33
0.29
0.33
Mature RNA/cell
Time (min)
n.s.
C
Active TS/cell
Active TS/cell
0 TS
1 TS
2 TS
>2 TS
Time (min)
D
NF-κB and nascent transcription dynamics
Nuclear NF-κB
Normalized nascent RNA/cell
Normalized nuclear NF-κB
Time (min)
NFKBIA
IL6
TNF
nuclear NF-κB

Figure 2

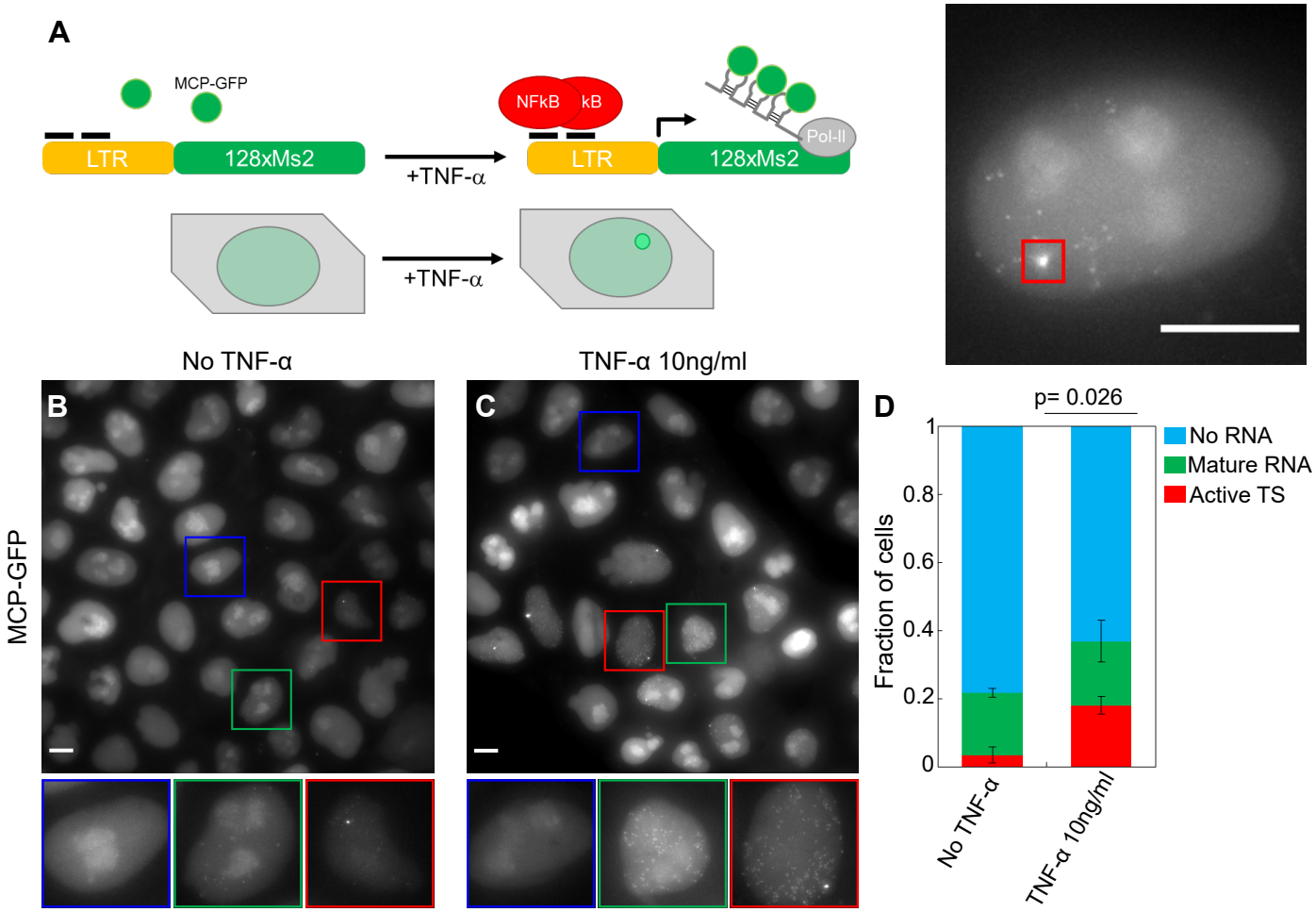
A
MCP-GFP
LTR
128xMs2
+TNF-α
NFkB
kB
Pol-II
No TNF-α
TNF-α 10ng/ml
MCP-GFP
B
C
D
p= 0.026
Fraction of cells
No RNA
Mature RNA
Active TS
No TNF-α
TNF-α 10ng/ml

Figure 3

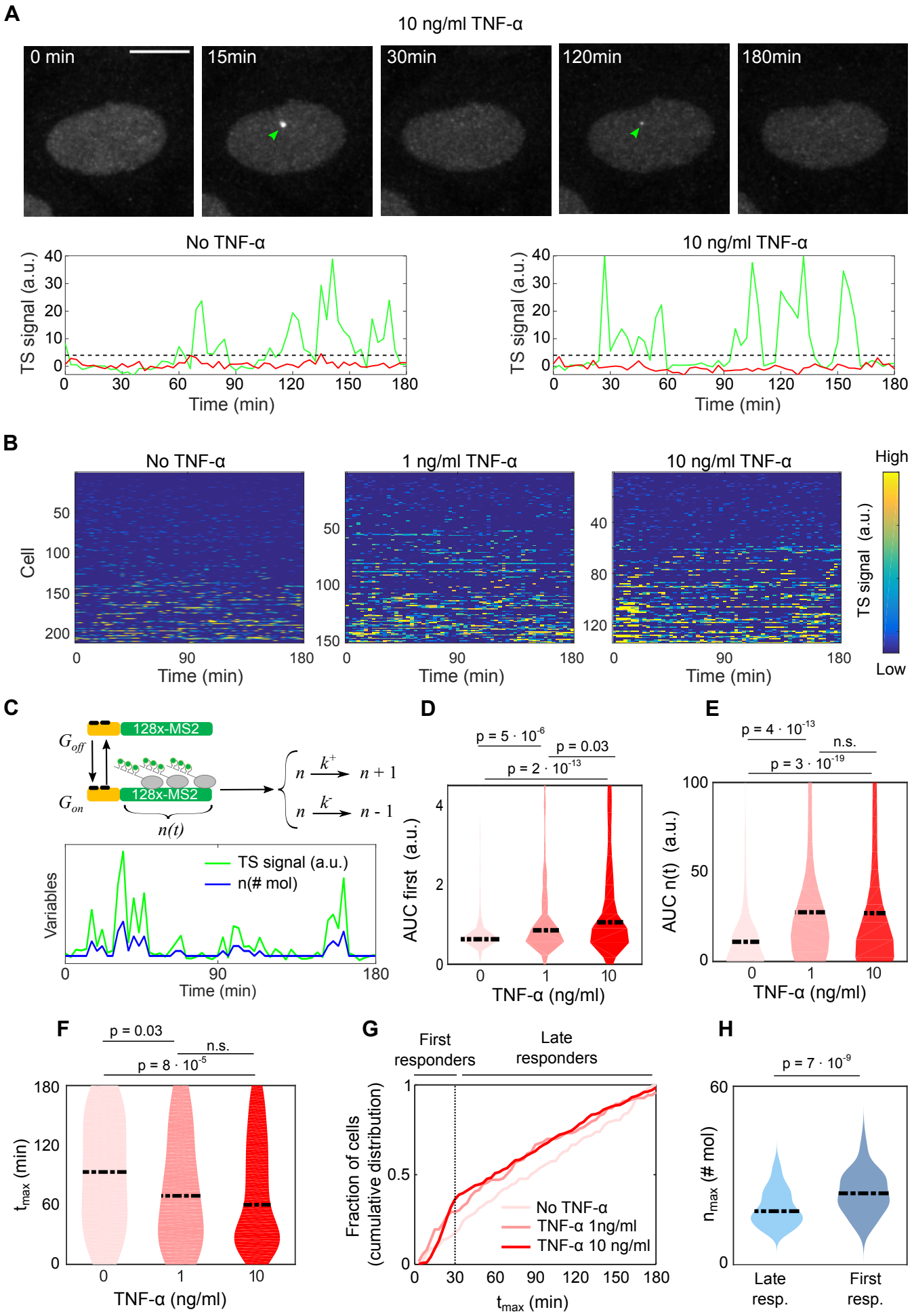
A
10 ng/ml TNF-α
0 min
15min
30min
120min
180min
No TNF-α
10 ng/ml TNF-α
TS signal (a.u.)
Time (min)
B
No TNF-α
1 ng/ml TNF-α
10 ng/ml TNF-α
Cell
Time (min)
High
Low
TS signal (a.u.)
C
128x-MS2
G_{off}
G_{on}
$n(t)$
$n \xrightarrow{k^+} n+1$
$n \xrightarrow{k^-} n-1$
Variables
TS signal (a.u.)
n(# mol)
Time (min)
D
p = 5 · 10^-6
p = 0.03
p = 2 · 10^-13
AUC first (a.u.)
TNF-α (ng/ml)
E
p = 4 · 10^-13
n.s.
p = 3 · 10^-19
AUC n(t) (a.u.)
TNF-α (ng/ml)
F
p = 0.03
n.s.
p = 8 · 10^-5
t_{max} (min)
TNF-α (ng/ml)
G
First responders
Late responders
Fraction of cells (cumulative distribution)
No TNF-α
TNF-α 1ng/ml
TNF-α 10 ng/ml
t_{max} (min)
H
p = 7 · 10^-9
n_{max} (# mol)
Late resp.
First resp.

Figure 4

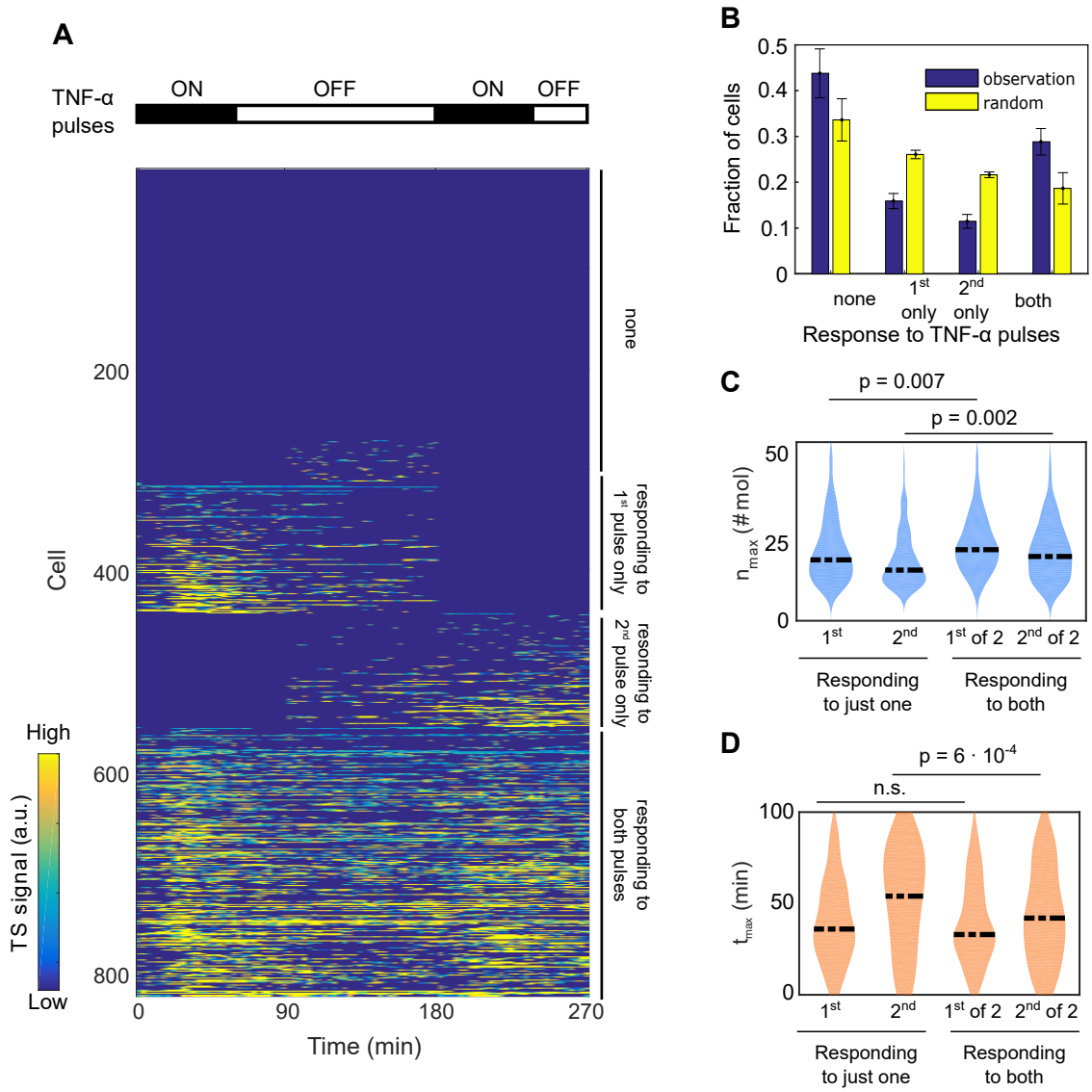
A
TNF-α pulses
ON
OFF
ON
OFF
Cell
200
400
600
800
0
90
180
270
Time (min)
High
Low
TS signal (a.u.)
none
responding to 1st pulse only
resonding to 2nd pulse only
responding to both pulses
B
Fraction of cells
0.5
0.4
0.3
0.2
0.1
0
observation
random
none
1st only
2nd only
both
Response to TNF-α pulses
C
p = 0.007
p = 0.002
n_max (# mol)
50
25
0
1st
2nd
1st of 2
2nd of 2
Responding to just one
Responding to both
D
p = 6 · 10^-4
n.s.
t_max (min)
100
50
0
1st
2nd
1st of 2
2nd of 2
Responding to just one
Responding to both

Figure 5

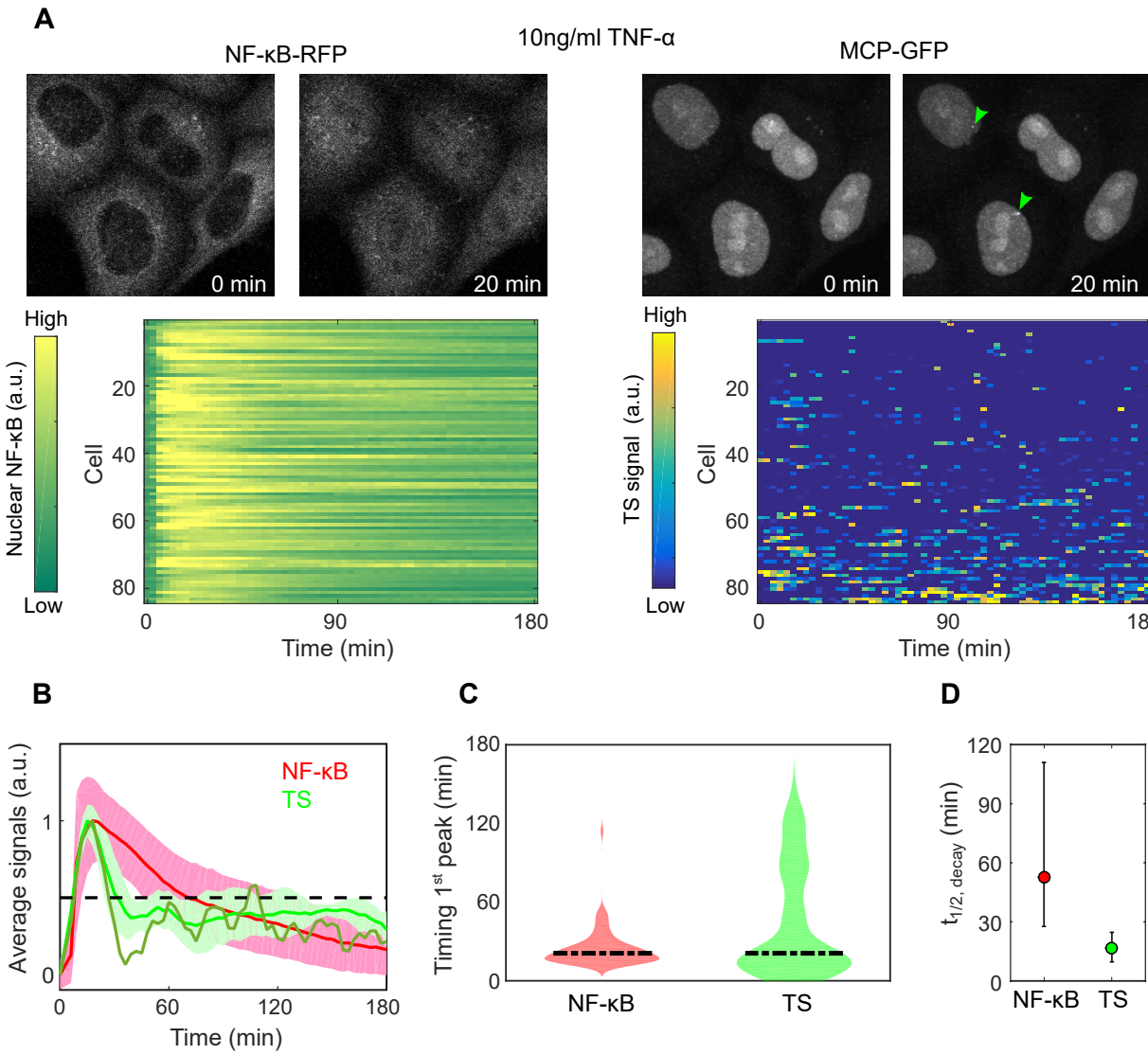
A
NF-κB-RFP
10ng/ml TNF-α
MCP-GFP
0 min
20 min
0 min
20 min
High
Low
Nuclear NF-κB (a.u.)
Cell
20
40
60
80
0
90
180
Time (min)
High
Low
TS signal (a.u.)
Cell
20
40
60
80
0
90
180
Time (min)
B
Average signals (a.u.)
NF-κB
TS
1
0
0
60
120
180
Time (min)
C
Timing 1st peak (min)
180
120
60
0
NF-κB
TS
D
$t_{1/2,\ decay}$ (min)
120
90
60
30
0
NF-κB
TS

Figure 6

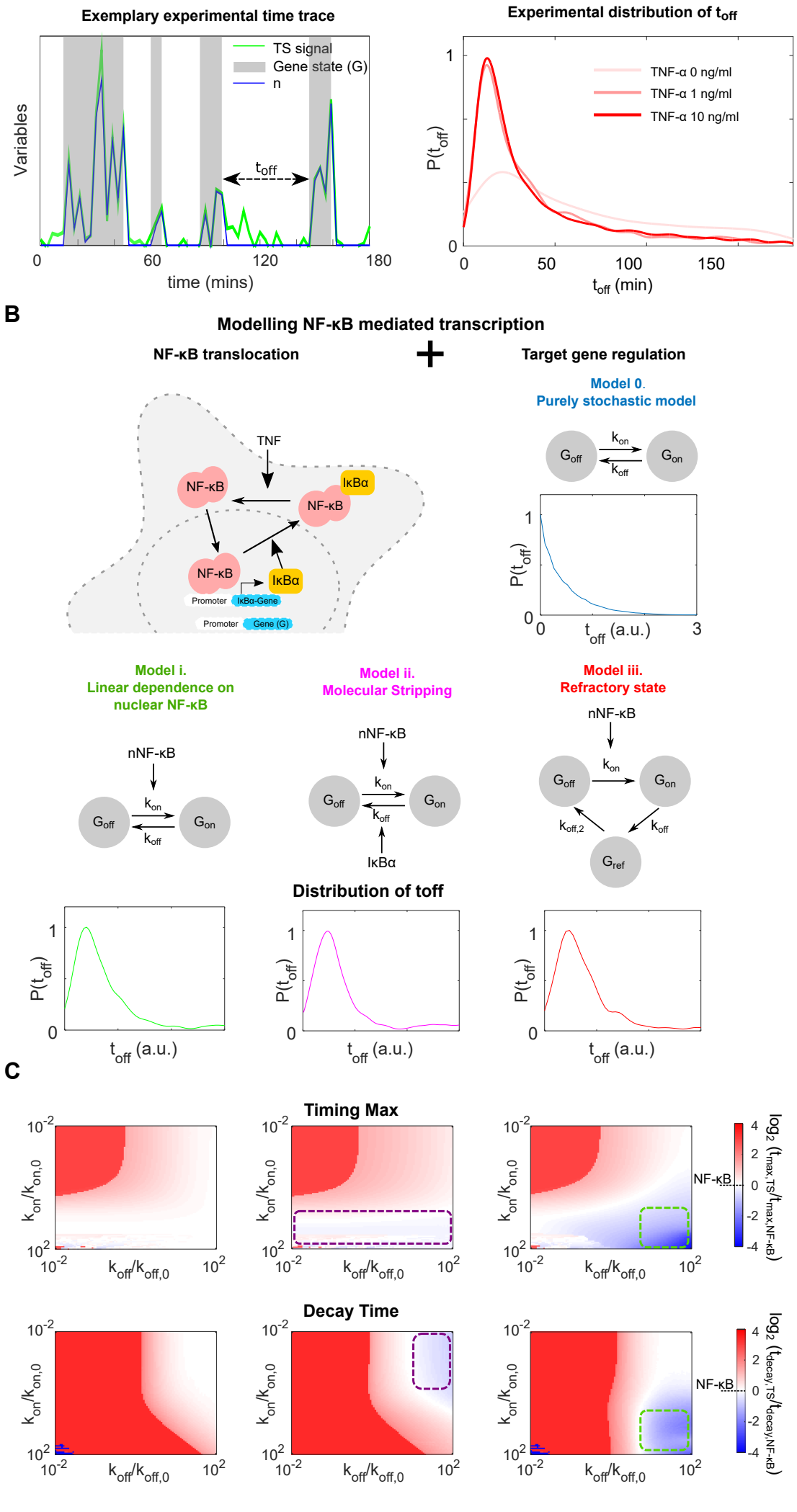
A
Exemplary experimental time trace
TS signal
Gene state (G)
n
Variables
t_{off}
0
60
120
180
time (mins)
Experimental distribution of t_{off}
TNF-α 0 ng/ml
TNF-α 1 ng/ml
TNF-α 10 ng/ml
$P(t_{off})$
1
0
0
50
100
150
t_{off} (min)
B
Modelling NF-κB mediated transcription
NF-κB translocation
+
Target gene regulation
TNF
NF-κB
IκBα
NF-κB
NF-κB
IκBα
Promoter
IκBα-Gene
Promoter
Gene (G)
Model 0.
Purely stochastic model
G_{off}
k_{on}
k_{off}
G_{on}
$P(t_{off})$
1
0
0
t_{off} (a.u.)
3
Model i.
Linear dependence on nuclear NF-κB
nNF-κB
k_{on}
G_{off}
G_{on}
k_{off}
Model ii.
Molecular Stripping
nNF-κB
k_{on}
G_{off}
G_{on}
k_{off}
IκBα
Model iii.
Refractory state
nNF-κB
k_{on}
G_{off}
G_{on}
$k_{off,2}$
k_{off}
G_{ref}
Distribution of toff
$P(t_{off})$
1
0
t_{off} (a.u.)
C
Timing Max
$k_{on}/k_{on,0}$
$k_{off}/k_{off,0}$
10^{-2}
10^{2}
NF-κB
$\log_2(t_{max,TS}/t_{max,NF-κB})$
4
2
0
-2
-4
Decay Time
$\log_2(t_{decay,TS}/t_{decay,NF-κB})$